REPORT DOCUMENTATION PAGE

1. REPORT DATE *(DD-MM-YYYY)*	2. REPORT TYPE	3. DATES COVERED *(From - To)*
29-07-2008	Final Phase 1	30-09-2007 to 29-06-2008

4. TITLE AND SUBTITLE
Technologies for Developing Predictive Atomistic and Coarse-Grained Force Fields for Ionic Liquid Property Prediction

5a. CONTRACT NUMBER
FA9550-07-C-0159

5b. GRANT NUMBER

5c. PROGRAM ELEMENT NUMBER

6. AUTHOR(S)
Marcus G. Martin, Edward J. Maginn, Robin D. Rogers, Greg Voth, Mark S. Gordon

5d. PROJECT NUMBER

5e. TASK NUMBER

5f. WORK UNIT NUMBER

7. PERFORMING ORGANIZATION NAME(S) AND ADDRESS(ES)
Useful Bias Incorporated
88 Martinez Road
Edgewood NM 87015-8222

8. PERFORMING ORGANIZATION REPORT NUMBER
0001AE

9. SPONSORING / MONITORING AGENCY NAME(S) AND ADDRESS(ES)
USAF, AFRL
AF OSR
875 N. Randolph St. Room 3112
Arlington VA 22203

10. SPONSOR/MONITOR'S ACRONYM(S)

11. SPONSOR/MONITOR'S REPORT NUMBER(S)
AFRL-SR-AR-TR-08-0515

12. DISTRIBUTION / AVAILABILITY STATEMENT
Approved for public release; distribution unlimited.

13. SUPPLEMENTARY NOTES

14. ABSTRACT
Report developed under STTR contract for topic AF07-T004: Force Fields for Modeling of Ionic Liquids. A force field was developed for the systems 1-Ethyl-1-methylpholinium Tricyanomethanide and 1-Ethyl-3-methylimidazolium Butanesulfonate using a combination of theoretical calculations and experimental data. The force field parameters simulation results are presented in this final report. In addition, experimental data on related ionic liquid systems is presented and discussed.

15. SUBJECT TERMS
STTR Report

16. SECURITY CLASSIFICATION OF:			17. LIMITATION OF ABSTRACT	18. NUMBER OF PAGES	19a. NAME OF RESPONSIBLE PERSON
a. REPORT	**b. ABSTRACT**	**c. THIS PAGE**			Marcus G. Martin
				23	**19b. TELEPHONE NUMBER** *(include area code)* (505) 286-4457

Standard Form 298 (Rev. 8-98)
Prescribed by ANSI Std. Z39.18

Simulation Subsection

GOAL

For Phase I, the goal of this project was to establish a protocol or pseudo-automated procedure for classical force field parameterization. The force field takes the form:

$$V_{tot} = \sum_{bonds} k_b(r - r_0)^2 + \sum_{angles} k_\theta(\theta - \theta_0)^2 + \sum_{dihedrals} k_\chi[1 + \cos(n\chi - \delta)] + \sum_{improper} k_\psi(\psi - \psi_0)^2 + \sum_{i}^{N-1}\sum_{j>i}^{N}\left\{ \varepsilon_{ij}\left[\left(\frac{r_{min,ij}}{r_{ij}}\right)^{12} - 2\left(\frac{r_{min,ij}}{r_{ij}}\right)^6\right] + \frac{q_i q_j}{r_{ij}}\right\}$$

$$V_{tot} = \sum_{bonds} k_b(r - r_0)^2 + \sum_{angles} k_\theta(\theta - \theta_0)^2 + \sum_{dihedrals} k_\chi[1 + \cos(n\chi - \delta)] + \sum_{improper} k_\psi(\psi - \psi_0)^2 + \sum_{i}^{N-1}\sum_{j>i}^{N}\left\{ \varepsilon_{ij}\left[\left(\frac{r_{min,ij}}{r_{ij}}\right)^{12} - 2\left(\frac{r_{min,ij}}{r_{ij}}\right)^6\right] + \frac{q_i q_j}{r_{ij}}\right\}$$

Parameters required include k_b, r_0, k_θ, θ_0, k_χ, n, δ, k_ψ, ψ_0, ε_{ij}, $r_{min,ij}$, q_i, q_j. A combination of *ab initio* electronic structure calculations (using GAMESS) and molecular mechanics calculations was used to optimize parameters for a user-specified molecule.

PHASE I PROGRESS/RESULTS
Test molecules:

(A) 1-Ethyl-1-methylphospholinium Tricyanomethanide
(some parameters for 1-ethyl-1-methylphospholinium cation taken from the work of Canongia Lopes and Padua)[1]

(B) 1-Ethyl-3-methylimidazolium Butanesulfonate
(some parameters for 1-ethyl-3-methylimidazolium cation taken from the work of Cadena et al).[2]

I. Intramolecular terms (bond, angles, dihedrals, impropers)

I.a. Bonds and Angles
The GAMESS[3] source code has been modified to punch optimized geometry parameters (r_0, θ_0) and the force constant matrix (containing the force constants k_b and k_θ) for a given molecule. The force constant matrix can be punched in internal coordinates (with appropriate units of *Hartree/Bohr^2* for bonds and *Hartree/rad^2* for angles) according to how the molecule was designated in the Z-matrix (not unique). A protocol is used to write 'intrinsic frequencies' corresponding to localized vibrational modes,[4] allowing one to extract intrinsic force constants for bond stretching only. These can be read directly into a formatted (i.e., CHARMM) force field. For the test molecules 1-Ethyl-1-methylphospholinium Tricyanomethanide and 1-Ethyl-3-methylimidazolium Butanesulfonate, the geometries were optimized at the B3LYP/TZVP level[5], and the force constants were used at this level, with appropriate scaling based on small molecule comparisons.[6]

Due to strong off-diagonal couplings in angle bending modes, the intrinsic force constants for angle bends will be more difficult to acquire, as their magnitudes in the force constant matrix are generally too high. This is evidenced in the example of the heterocyclic cation 1-butyl-3-methylimidazolium, for which the diagonal force constant element for the N–C–N ring angle is punched to be ~3 Hartree/rad^2, with several off-diagonal couplings of the same magnitude. This may be rationalized due to restrictive ring constraints. This issue is also relevant to other systems where dependent angle bending modes exist. A solution is required for this problem, such as making the force constant matrix as diagonal as possible, thus generating the most localized force constants possible. In addition, judicious choice of internal coordinates is required, as different initial Z-matrices or poorly chosen coordinates may produce different or erroneous results. For most systems, the diagonal angle force constants may possibly be used, with the qualification that they are probably an upper-bound to the true values. The quality of the force constants used must necessarily go hand-in-hand with the desired result. If the calculated property is only minimally dependent on the intramolecular parameters (i.e., static properties), then

the amount of effort imparted to achieve the desired outcome must be evaluated. Due to these challenges, the angle force constants were derived by performing structural perturbations on smaller related molecules where the angles were incremented by -2 to 2°, followed by single point energy calculations at the B3LYP/TZVP level. The force constants were derived assuming a harmonic approximation and averaged.

GAMESS-specific required flags and brief description:
$statpt   hssend = .t.   (compute hessian at stationary point)
$force   vibanl = .t.   (perform vibrational analysis)
                  decomp = .t. (activates internal coordinate frequency analysis)
                  prtifc = .t.   (print internal force constants)
                  puncff = .t. (print force field information at end of log file)

(Note: The *puncff* flag was specifically added for this project).

I.b. **Dihedrals**

Dihedral analysis and parameterization requires a combination of *ab initio* calculations and molecular mechanics calculations. A perl script has been written (***torsion.pl***) to generate a series of GAMESS input files for dihedral scan analysis. The optimized geometry for a given molecule (performed previously in section *I.a.*) is placed into a GAMESS input file (i.e., example.inp). The geometry must be specified in Z-matrix form. Additionally, the user must set a flag corresponding to the particular dihedral that will be scanned and held fixed during the constrained optimization.

GAMESS-specific required flag needed for the perl script (and description):
$statpt   ifreeze(1) = **x** (x is numerical reference to the particular internal
                                  dihedral coordinate to be scanned as defined in Z-matrix)

The perl script is executed as follows for the example.inp case file:

./**torsion.pl** example.inp **y** example.d####

The variable **y** indicates the exact line of the Z-matrix containing **x** (noting that all lines containing flags are ignored by the script). The perl script creates a series of input files (containing the flags listed in example.inp) in which the particular dihedral (**x**) to be scanned in the molecule has been rotated in +10° increments. The files created are of the type as shown below, where #### are the specific atoms labels in the dihedral:

example.d####+10.inp, example.d####+20.inp, … , example.d####+360.inp

If a series of unique dihedral angles are present in the molecule, individual example.inp files must be created with the unique ifreeze(1) numerical references specified, and the perl script is run for each of these to create the scan files. A system-specific batch submission script may be written to run these GAMESS input files.

It is general practice in force field development to run constrained optimization scans at a low to moderate level of theory. Following the scan, the optimized geometries at each scan point must then be extracted and reinserted into new GAMESS input decks in which the theory level has been modified to obtain proper energetics as a function of dihedral angle. For the anions of test molecules of (A) and (B), appropriate dihedral scans were performed at the B3LYP/TZVP level of theory. It was found that these profiles closely matched those calculated at the MP2(FC)/cc-pVTZ(-f) level, where (-*f*) means that f-type functions have been removed from the basis set.[7]

Following the ab initio analysis, a molecular mechanics (MM) analysis is also required. Here, the B3LYP/TZVP optimized geometries are also extracted and inserted into .pdb files (protein databank files) or other coordinate files. The .pdb files are commonly used in various MM packages such as CHARMM8 or

NAMD9. Connectivity must also be specified, and tools exist to create proper connectivity files (as well as to create .pdb files). From here, relaxed MM energies may be obtained using a force field in which the particular dihedral parameters begin studied are set to zero and a constrained MM minimization is performed. It is critical that all other force field parameters (for bonds, angles, charges, and Lennard-Jones interactions) be pre-specified. The MM energies are then subtracted from the *ab initio* energies, and the resultant curve is then fit to a cosine series using non-linear regression tools. The number of terms in the cosine series is varied to obtain the best possible fit the data.

Challenges that still remain for obtaining dihedral force field parameters mainly involve automating the step-wise procedure of ab initio scan, MM scan, subtraction, and non-linear regression as described above. However, all of the tools are in place to reach the goal and proof-of-concept may be demonstrated with a well-defined procedure, and automation of this step may be implemented at a later date. A significant challenge remains for the treatment of ring systems (particularly ionic liquids), since scanning of the ring dihedrals may produce unphysical results. In this case, identifying the symmetry of the problem and tailoring the parameterization accordingly may be critical.

For Phase I, the above described procedure was performed manually to obtain dihedral parameters for the anions of (A) and (B). Dihedral parameters for the cation of (B) were taken directly from the work of Cadena et al.2 Dihedral parameters for the cation of (A) were derived from the work of Canongia Lopes and Padua1 for linear phosphonium cations and applied to the cyclic pholinium system.

II. Intermolecular terms (Point charges, Lennard-Jones parameters)

II.a. Point Charges
As atomic centered charges are not quantum-mechanical observables, many procedures exist to assign these charges from *ab initio* electronic structure calculations. Force field charges are primarily assigned using the CHELPG procedure,10 in which the electrostatic potential, calculated at a particular level of theory, is projected onto the atomic sites, such that the gas-phase dipole moment of the molecule is conserved. Charges for the cations and anions of (A) and (B) were calculated at the MP2/cc-pVTZ(-f)//B3LYP/TZVP level of theory.11 GAMESS is equipped to routinely calculate CHELPG charges.

GAMESS-specific required flags and brief description:
$elpot	iepot = 1	(initialize electrostatic potential calculation)
	where = pdc	(type of calculation)
$pdc	ptsel = chelpg	(calculate chelpg charges)
	constr = dipole	(constraint to reproduce the dipole moment)

(Note: The *puncff* flag described above will punch the chelpg charges at end of file).

II.b. Lennard-Jones Parameters
Lennard-Jones (LJ) parameter assignment and optimization poses the most significant challenge to an automated force field generation protocol. Moderately complex procedures exist to obtain LJ parameters from *ab initio* electronic structure calculations. For example, an atom with well-known LJ parameters (i.e., Ar) is moved along the surface of a molecule, and at particular locations, the interaction energies are calculated (high level calculations are required). Assuming a given set of mixing rules and a defined mathematical form for the interaction potential, the LJ parameters may be obtained using appropriate fitting procedures. Automation of the LJ parameterization using a similar protocol is an appropriate goal for Phase II/Phase III of the project. Currently, the protocol involves extracting LJ parameters from predefined force fields (i.e., CHARMM, Amber) or literature sources for the atoms in similar chemical environments as exist if the user-defined molecule. For example, an ionic liquid containing a ether group in the alkyl chain potion of the molecule would require LJ parameters for oxygen in a similar environment as described in another force field. Due to the vast amount of force field data that exists in the scientific community, ample opportunity is present to tabulate much of the data

and obtain the best possible set of LJ parameters for a diversity of atom types to be used in Phase I of the automation procedure. We are currently developing a *force field database* from which appropriate LJ parameters can be found from compiled literature sources. LJ parameters for the anions were taken from the CHARMM force field8 for similar atom types, and the LJ parameters for the cation were taken from literature sources.1[,2] A beta version of the database exists at: http://www.nd.edu/~lmmr

GAMESS possess the capability to calculate the Lennard-Jones parameters using an entirely first principles approach, thus allowing for the development of internally consistent values for force field work and eliminating the need to pick and choose literature values. Here, an effective fragment potential (EFP) method is used to develop interaction potentials based on localized orbitals. Thus, tools are available for the parameterization using electronic structure theory, and require projection of the localized orbital values onto the atoms to achieve the desired parameters. This approach is considered to be a Phase II/Phase III objective.

It is noted that force field parameters may be refined in particular cases based on comparisons to available experimental data. For example, comparison of simulated liquid densities or heats of vaporization to experimental values may warrant refinement of the $r_{min,ij}$ or ε_{ij} values. These properties are to a large extent decoupled and therefore the LJ parameters may be refined fairly independently of one another. It is also noted that this refinement requires the user to evaluate the quality of the simulation data, and involves a greater amount of user intervention than would be required for the general force field development procedure described herein.

III. Other Considerations

The above outlined strategic approach to force field parameterization will be immensely beneficial to the ionic liquid community in the development of new ionic liquids for specific tasks and the evaluation of their properties. The tremendous number of possible ionic liquids that are within reach makes it critical that a reliable approach is available to guide experimental efforts and design. In addition, the automation of force field development will also be beneficial to other fields, as the approach in not restricted to ionic liquids. The ability to have reliable force field at one's fingertips for the study of materials that exhibit non-linear optical properties or for materials that contain transition metals, lanthanides, and actinides will also have a positive impact in the simulation community.

PHASE I PROTOCOL OVERIEW: CONCLUSIONS

1. DEFINE AND DRAW MOLECULE TO BE PARAMETERIZED
    a. Use wxMacMolPlot (version 7.0b3)
    b. Define a Z-matrix for the molecule. Use a Z-matrix that captures the largest number of required parameters
    c. Assign individual atom types consistent with force field development

2. OPTIMIZE EQUILIBRIUM GEOMETRY AND CALCULATE VIBRATIONAL FREQUENCIES OF MOLECULE USING GAMESS
    a. Use consistent level of theory, as common in force field development
    b. Screen for imaginary modes; if present, modify geometry and try again
    c. Use appropriate GAMESS flags to punch force field information

3. EXTRACT BOND DISTANCES AND ANGLES AND CORRESPONDING FORCE CONSTANTS FROM GAMESS OUTPUT
    a. Use intrinsic force constants for bonds
    b. Use diagonal elements of internal force constant matrix for angles
    c. Check for presence of ring, and assign force field parameters accordingly
    d. Repeat steps 1-3 for internal coordinates that were missing from original Z-matrix, since not all internals are necessarily uniquely defined
    e. Export values to force field parameter file (.PRM) in appropriate format (i.e., CHARMM)

4. EXTRACT CHELPG ATOMIC CHARGES FROM GAMESS OUTPUT
    a. Compare CHelpG dipole with ab initio dipole to ensure agreement
    b. Export values to force field connectivity file (.PSF) in appropriate format (i.e., CHARMM)

5. ASSIGN LJ PARAMETERS FROM TABULATED DATA
    a. Read atoms types defined in step 1c and identify corresponding LJ parameters
    b. Export values to force field parameter file (.PRM) in appropriate format (i.e., CHARMM)
    c. Use GAMESS EFP method when available

6. PERFORM AB INTIO DIHEDRAL OPTIMIZATION SCANS AND ENERGETICS SCANS
    a. Create GAMESS input file with appropriate flags and Z-matrix corresponding to optimized geometry obtained in 2a.
    b. Identify dihedral angle to scan (internal coordinate number and Z-matrix line number)
    c. Run torsion.pl script on this input file to create series of GAMESS scan files (36 total)
    d. Use batch submission script to run each GAMESS constrained optimization calculation where assigned dihedral coordinate is kept fixed
    e. Extract optimized coordinates from each of the 36 scan files and export into 36 new GAMESS input files for high level B3LYP/TZVP or MP2/cc-pVTZ(-f) energy calculations
    f. Use batch submission script to run each GAMESS single point energy calculation where geometry is kept fixed
    g. Plot energy vs. dihedral angle to observe periodicity and check for problems

7. PERFORM MOLECULAR MECHANICS DIHEDRAL RELAXATION SCANS (EXAMPLE W/ NAMD)
    a. Extract optimized coordinates from each of the 36 scan files (6d) and export into 36 new .PDB files for MM energy calculations
    b. Define molecular connectivity in .PSF file
    c. Define MM simulation details in .CONF file, including temperature (0 K), constraints (dihedral), and minimization steps

d. Confirm that force field file (.PRM) is complete, with dihedral parameters set to zero for dihedral being studied
e. Use batch submission script to run each NAMD minimization calculation, where all other degrees of freedom allowed to relax
f. Plot energy vs. dihedral angle to observe periodicity and check for problems

8. PERFORM SUBTRATION AND COSINE SERIES FIT
a. Subtract curve 7f from curve 6g to obtain energy vs. dihedral angle curve to be fit with cosine series
b. Use nonlinear regression to obtain best fit cosine series parameters, where the number of terms in the series is altered to obtain ideal fit
c. Export values to force field parameter file (.PRM) in appropriate format (i.e., CHARMM)
d. Repeat steps 6 to 8 for all dihedrals to be fit, keeping in mind that the ideal parameterization procedure may be a 'building-up' procedure (Pádua, *J. Phys. Chem. A* **2002**, *16*, 10116), starting with smaller molecules of similar chemical composition OR may require appropriate dihedral constraints/restraints.

9. RUN SIMULATIONS AND REFINE FORCE FIELD IF NECESSARY
a. Run molecular simulation (Molecular Dynamics or Monte Carlo) using newly parameterized force field.
b. Compare several calculated properties (i.e., liquid density, heat of vaporization) with available experimental data and evaluate quality of force field
c. If necessary, refine the LJ parameters and repeat steps 5-8.

FORCE FIELDS DEVELOPED FOR TEST ILs (A) and (B)

(A) 1-Ethyl-1-methylpholinium Tricyanomethanide
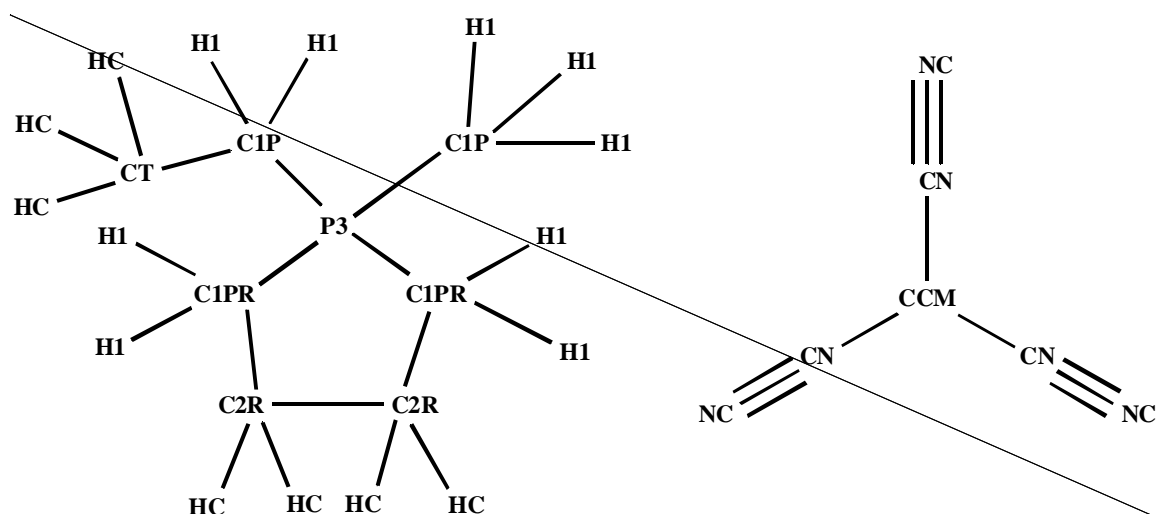
Bonds

Atom1	Atom2	k$_r$	r$_0$
P3	C1P	206.0	1.823
P3	C1PR	206.0	1.839
C1PR	C2R	281.0	1.547
C2R	C2R	281.0	1.538
C1P	CT	281.0	1.534
C1P	H1	340.0	1.092
C1PR	H1	340.0	1.092
C2R	HC	340.0	1.092
CT	HC	340.0	1.092
CCM	CN	430.0	1.408
CN	NC	1210.0	1.167

Angles

Atom1	Atom2	Atom3	k$_\theta$	θ_0
C1PR	P3	C1PR	58.0	97.1
C1P	P3	C1P	58.0	108.6
C1PR	P3	C1P	58.0	112.8
P3	C1PR	C2R	55.0	104.2
P3	C1PR	H1	42.0	109.8
P3	C1P	H1	42.0	108.4
P3	C1P	CT	55.0	115.2
C1PR	C2R	C2R	67.0	107.9
H1	C1PR	C2R	45.0	112.6
H1	C1PR	H1	35.0	108.7
H1	C1P	H1	35.0	108.5
HC	C2R	C1PR	45.0	110.1
HC	C2R	C2R	45.0	110.9
HC	C2R	HC	35.0	107.0
H1	C1P	CT	45.0	111.0
HC	CT	C1P	45.0	111.1
HC	CT	HC	35.0	107.8

NC	CN	CCM	30.0	179.999
CN	CCM	CN	44.0	120.0

Dihedrals

Atom1	Atom2	Atom3	Atom4	k_χ	n	δ
C2R	C1PR	P3	C1PR	0.1354	3	0
C2R	C1PR	P3	C1P	0.1354	3	0
H1	C1PR	P3	C1PR	0.1108	3	0
H1	C1PR	P3	C1P	0.1108	3	0
C2R	C2R	C1PR	P3	-0.3882	1	0
C2R	C2R	C1PR	P3	0.1181	2	180
C2R	C2R	C1PR	P3	-0.0854	3	0
C2R	C2R	C1PR	H1	0.1830	3	0
HC	C2R	C1PR	P3	0.0556	3	0
HC	C2R	C1PR	H1	0.1590	3	0
C1PR	C2R	C2R	C1PR	0.8700	1	0
C1PR	C2R	C2R	C1PR	-0.0785	2	180
C1PR	C2R	C2R	C1PR	0.1395	3	0
HC	C2R	C2R	C1PR	0.1830	3	0
HC	C2R	C2R	HC	0.1590	3	0
CT	C1P	P3	C1P	0.1354	3	0
CT	C1P	P3	C1PR	0.1354	3	0
H1	C1P	P3	C1P	0.1108	3	0
H1	C1P	P3	C1PR	0.1108	3	0
HC	CT	C1P	P3	0.0556	3	0
HC	CT	C1P	H1	0.1590	3	0
NC	CN	CCM	CN	0.0000	2	180

Impropers

Atom1	Atom2	Atom3	Atom4	k_ψ	ψ_0
CCM	CN	CN	CN	26.7	0

Lennard-Jones

Atom	ε (kcal/mol)	$R_{min}/2$ (Å)	ε, 1,4 (kcal/mol)	$R_{min}/2$, 1,4 (Å)
P3	-0.200	2.09900	-0.100	2.09900
C1P	-0.066	1.96431	-0.033	1.96431
C1PR	-0.066	1.96431	-0.033	1.96431
C2	-0.066	1.96431	-0.033	1.96431
C2R	-0.066	1.96431	-0.033	1.96431
CS	-0.066	1.96431	-0.033	1.96431
CT	-0.066	1.96431	-0.033	1.96431
H1	-0.030	1.40308	-0.015	1.40308
HC	-0.030	1.40308	-0.015	1.40308
CCM	-0.080	1.99000	-0.040	1.99000
CN	-0.200	1.75000	-0.100	1.75000
NC	-0.600	1.85000	-0.300	1.85000

Point charges

Atom	q	Position
C2R	0.002673	ring
C1PR	-0.11372	ring
HC	0.042066	ring
H1	0.077653	ring
P3	0.524067	ring
C1P	-0.448522	methyl
H1	0.169514	methyl
C1P	-0.061952	ethyl
H1	0.080296	ethyl
CT	-0.211279	ethyl
HC	0.09059	ethyl
CCM	-0.651445	anion
CN	0.578642	anion
NC	-0.694827	anion

(B) 1-Ethyl-3-methylimidazolium Butanesulfonate
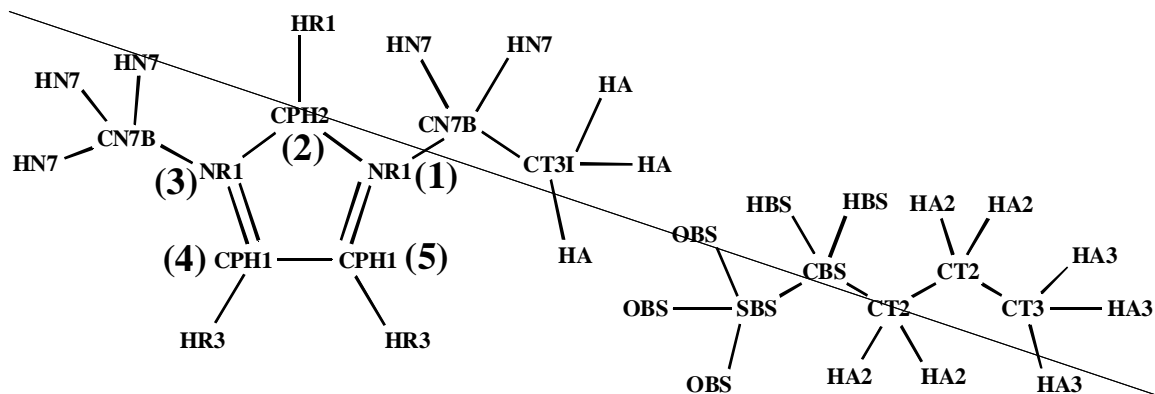
Bonds

Atom1	Atom2	k_r	r_0
CPH1	CPH1	410.0	1.361
NR1	CPH2	400.0	1.337
NR1	CPH1	400.0	1.382
NR1	CN7B	220.0	1.477
CPH1	HR3	365.0	1.077
CPH2	HR1	340.0	1.078
CN7B	HN7	309.0	1.090
CN7B	CT3I	200.0	1.524
CT3I	HA	322.0	1.092
CBS	HBS	346.6	1.093
CBS	SBS	178.6	1.842
SBS	OBS	528.5	1.492
CBS	CT2	298.5	1.523
CT2	HA2	331.0	1.096
CT2	CT2	287.8	1.534
CT2	CT3	292.5	1.532
CT3	HA3	337.0	1.095

Angles

Atom1	Atom2	Atom3	k_θ	θ_0
NR1	CPH1	CPH1	130.0	107.18
CPH1	NR1	CPH2	130.0	108.28
NR1	CPH2	NR1	130.0	109.08
CPH2	NR1	CN7B	130.0	125.88
CPH1	NR1	CN7B	130.0	125.83
HN7	CN7B	NR1	30.0	108.33
HN7	CN7B	HN7	35.5	108.97
HR1	CPH2	NR1	25.0	125.46
HR3	CPH1	NR1	25.0	122.09
HR3	CPH1	CPH1	25.0	130.73
HN7	CN7B	CT3I	33.4	111.69
HA	CT3I	CN7B	33.4	110.86
HA	CT3I	HA	35.5	108.03
NR1	CN7B	CT3I	140.0	112.44
HBS	CBS	SBS	37.0	105.69
HBS	CBS	HBS	33.0	108.55

OBS	SBS	CBS	74.0	104.35
OBS	SBS	OBS	95.6	114.07
SBS	CBS	CT2	61.6	112.97
HBS	CBS	CT2	45.0	111.77
HA2	CT2	CBS	45.0	108.79
HA2	CT2	HA2	35.0	106.20
HA2	CT2	CT2	45.0	109.59
CBS	CT2	CT2	53.4	113.23
HA2	CT2	CT3	45.0	109.33
HA3	CT3	CT2	45.0	111.26
HA3	CT3	HA3	35.0	107.62
CT3	CT2	CT2	53.4	113.14

Dihedrals

Atom1	Atom2	Atom3	Atom4	k_χ	n	δ
NR1	CPH1	CPH1	NR1	14.0000	2	180
HR3	CPH1	CPH1	NR1	3.0000	2	180
HR3	CPH1	CPH1	HR3	2.0000	2	180
CPH1	NR1	CPH2	NR1	14.0000	2	180
CPH1	NR1	CPH2	HR1	3.0000	2	180
CN7B	NR1	CPH2	NR1	0.0000	1	0
CN7B	NR1	CPH2	HR1	0.0000	1	0
CPH1	CPH1	NR1	CPH2	14.0000	2	180
HR3	CPH1	NR1	CPH2	3.0000	2	180
CPH1	CPH1	NR1	CN7B	0.0000	1	0
HR3	CPH1	NR1	CN7B	0.0000	1	0
CPH2	NR1	CN7B	HN7	0.1950	2	180
CPH1	NR1	CN7B	HN7	0.0000	1	0
CPH2	NR1	CN7B	CT3I	0.1000	3	180
CPH1	NR1	CN7B	CT3I	0.2000	4	0
HA	CT3I	CN7B	NR1	0.0000	3	0
HA	CT3I	CN7B	HN7	0.1950	3	0
OBS	SBS	CBS	HBS	0.1758	3	0
OBS	SBS	CBS	CT2	0.1963	3	0
HA2	CT2	CBS	HBS	0.1540	3	0
HA2	CT2	CBS	SBS	0.1021	3	0
CT2	CT2	CBS	HBS	0.1842	3	0
CT2	CT2	CBS	SBS	-1.6288	1	0
CT2	CT2	CBS	SBS	-0.2844	2	180
CT2	CT2	CBS	SBS	0.1040	3	0
HA2	CT2	CT2	HA2	0.1540	3	0
HA2	CT2	CT2	CBS	0.1842	3	0
CT3	CT2	CT2	HA2	0.1842	3	0
CT3	CT2	CT2	CBS	0.5218	1	0
CT3	CT2	CT2	CBS	-0.0826	2	180
CT3	CT2	CT2	CBS	0.2002	3	0
CT3	CT2	CT2	CBS	-0.1348	4	180
HA3	CT3	CT2	HA2	0.1540	3	0
HA3	CT3	CT2	CT2	0.1842	3	0

Impropers

Atom1	Atom2	Atom3	Atom4	k_ψ	ψ_0
CPH2	NR1	NR1	HR1	0.5	0
NR1	CPH1	CPH2	CN7B	0.6	0
CPH1	CPH1	NR1	HR3	0.5	0

Lennard-Jones

Atom	ε (kcal/mol)	$R_{min}/2$ (Å)	ε, 1,4 (kcal/mol)	$R_{min}/2$, 1,4 (Å)
CPH1	-0.050	1.800	-0.025	1.800
CPH2	-0.050	1.800	-0.025	1.800
NR1	-0.200	1.850	-0.100	1.850
CT3I	-0.055	2.175	-0.028	2.175
CN7B	-0.020	2.275	-0.010	2.275
HR1	-0.046	0.900	-0.023	0.900
HR3	-0.008	1.468	-0.004	1.468
HA	-0.022	1.320	-0.011	1.320
HN7	-0.022	1.320	-0.011	1.320
HA3	-0.024	1.340	-0.012	1.340
CT3	-0.078	2.040	-0.039	2.040
CT2	-0.056	2.010	-0.028	2.010
HA2	-0.028	1.340	-0.014	1.340
SBS	-0.470	2.100	-0.235	2.100
OBS	-0.120	1.700	-0.060	1.700
CBS	-0.056	2.010	-0.028	2.010
HBS	-0.028	1.340	-0.014	1.340

Point charges

Atom	q	Position
NR1	0.059039	N(1)
CPH2	-0.091254	C(2)
NR1	0.193632	N(3)
CPH1	-0.147496	C(4)
CPH1	-0.13447	C(5)
HR1	0.218924	H-C(2)
HR3	0.210036	H-C(4)
HR3	0.220283	H-C(5)
CN7B	-0.249056	methyl
HN7	0.144661	methyl
CN7B	0.104248	ethyl
HN7	0.055487	ethyl
CT3I	-0.104508	ethyl
HA	0.058555	ethyl
CT3	-0.239807	anion
HA3	0.033959	anion
CT2	0.216198	anion, adj CT3
HA2	-0.06086	anion, adj CT3
CT2	0.183302	anion, adj CBS
HA2	-0.026246	anion, adj CBS
CBS	-0.32711	anion
HBS	0.067128	anion
SBS	1.385025	anion

| OBS | -0.759843 | anion |

CALCULATED PROPERTIES

Results

(A) 1-Ethyl-1-methyl-pholinium Tricyanomethanide

Liquid density (calculated)
ρ (g/cm^3): 1.062

Self-diffusion coefficient (calculated)
D_s (cation, m^2/s) : 1.08 x 10^{-13}
D_s (anion, m^2/s) : 1.72 x 10^{-13}

(B) 1-Ethyl-3-methylimidazolium Butanesulfonate

Liquid density (calculated)
ρ (g/cm^3): 1.133

Self-diffusion coefficient (calculated)
D_s (cation, m^2/s) : 2.72 x 10^{-12}
D_s (anion, m^2/s) : 1.45 x 10^{-12}

Experimental Subsection

A. Project Justification and Synthetic Target Selection:

Hydrazinium Salts as Potential Energetic Material Candidate:

Hydrazinium-based ionic liquids (ILs) have been selected as potential candidates for use in propulsion applications, as it has been demonstrated previously that such compounds can be successfully utilized as propellants.[12, 13] Additionally, as ionic liquids, these compounds are found to bear other favorable properties that are less frequently observed for materials of strictly molecular (non-ionic) nature: (i) relative insensitivity to frictional stress and electrostatics, (ii) negligible volatility due to very low vapor pressures, and (iii) relatively good thermal stability. Additionally, due to the ionic liquid nature of these materials they have advantage of broad liquidus ranges and the potential for dual-functionalization of either component anion or cation.

2-Hydroxyethyl-Hydrazinium Salts: Justification for the choice of the specific cation for investigation:

Salts based on the parent structure of the neutral 2-hydroxyethyl-hydrazine (HEH) have been previously reported by Brand and Drake, where it was anticipated that the addition of the 2-hydroxyethyl side-chain would result in reduced volatility in comparison to hydrazine.[14]   Such salts have been chosen as the subjects for a computational investigation, and the objective for the team here at The University of Alabama is to serve as the center for the synthesis of chosen targets and to provide all needed data that will support the computationally modeled systems.

2-Hydroxyethyl-Hydrazinium Salts: Targeted 1:1 and 1:2 salts

The mono- and diprotic salts of hydrazinium have been selected as specific mono- and dianionic targets, respectively, and they are obtained by protonation of HEH with a broad array of common Brönsted acids (Figure 1):
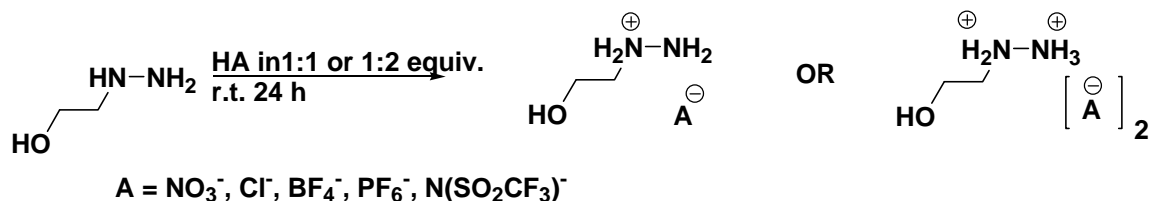
Figure 1. Mono- and diprotonation of 2-hydroxyethyl-hydrazine by addition of common Brönsted acids

♦ The synthetic targets generated will permit comparison of change in anion identity as well as comparison of mono- and dicationic salts.
♦ Perchlorate (ClO_4^-) was originally indicated as a potential target, but it has been removed from the current set due to potential instability issues in handling the material.

B. Experimental Section:

Work Plan and Status:

♦ Synthesize 2-hydroxyethyl-hydrazinium salts in 1:1 and 1:2 ratios (cation:anion) as ~ 1.5 gram sample:
  o Nitrate (NO_3^-) [DONE]
  o Chloride (Cl^-) [DONE]
  o Tetrafluoroborate (BF_4^-) [DONE]
  o Hexafluorophosphate (PF_6^-) [DONE]
  o Bistrifylamide (NTf_2^-) [DONE]
  o Perchlorate (ClO_4^-) [Target postponed, see last section]

♦ Characterize the physical properties of the samples:
  o 1H-NMR [DONE]
  o Karl-Fischer / FT-IR (determination of purity)
  o TGA: (T_{onset}, $T_{5\% dec}$, T_{dec}) [DONE]
  o DSC (T_m, T_g, T_{cryst}, etc.) [DONE]
  o Heat capacity (C_p)
  o Thermal Stability (24 hour @ 75 ^{o}C isothermal) [DONE]
  o XRD

♦ Make one salt in 5 gram scale (e.g., 2-OHET-HY [NO_3] [DONE]
♦ Order 2-OHEt-HY from Aldrich [DONE]

General Synthetic Approach for the formation of 2-hydroxyethyl-hydrazinium (1:1) salts:

The acids were used as concentrated aqueous solutions in reaction with 2-hydroxyethyl-hydrazine (Fluka, 98%) as purchased. To a 20 mL glass vial, the 2-hydroxyethyl hydrazine (10 mmol, 0.7610 g) was added followed by the addition of acid (10 mmol). The vials were capped and then stirred overnight, followed by ~12 hours drying in air at 50 ^{o}C furnace.

General Synthetic Approach for the formation of 2-hydroxyethyl-hydrazinium (1:2) salts:

The procedure here is similar to that described above for the 1:1 salts, except that the amount of acid used is increased to 20 mmol.

General Synthetic Approach for the formation of 5 gram scale-up of 2-hydroxyethyl-hydrazinium nitrate (1:1) salt:

The synthesis for the 5 gram scale up of the 2-OHEt-HY[NO$_3$] salt is similar to the synthesis of other 1:1 salts described above, with the change in both starting materials to 50 mmol quantities and the use of a 50 mL round-bottom flask as the reaction vessel.
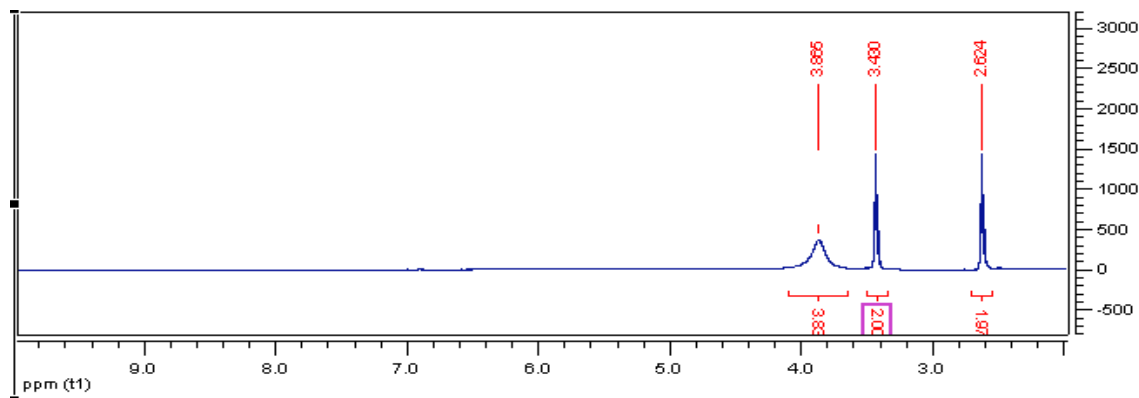
X. <u>Results and Discussion:</u>

Part A: ^{1}H-NMR

Figure A1: ^{1}H-NMR plot for 2-hydroxyethyl hydrazine (neutral) salt precursor; 360 MHz DMSO-d_6

♦ Highly shielded amine and hydroxy proton signal (δ ~ 3.865) is accurate for integration of approximately 4H = (2H$_{NH2}$ + 1H$_{NH}$ + 1H$_{OH}$).

♦ -CH$_2$OH (δ = 3.430 ppm) and –CH$_2$NH (δ = 2.624 ppm) appear as triplets at the expected integration and chemical shift compared with literature values.
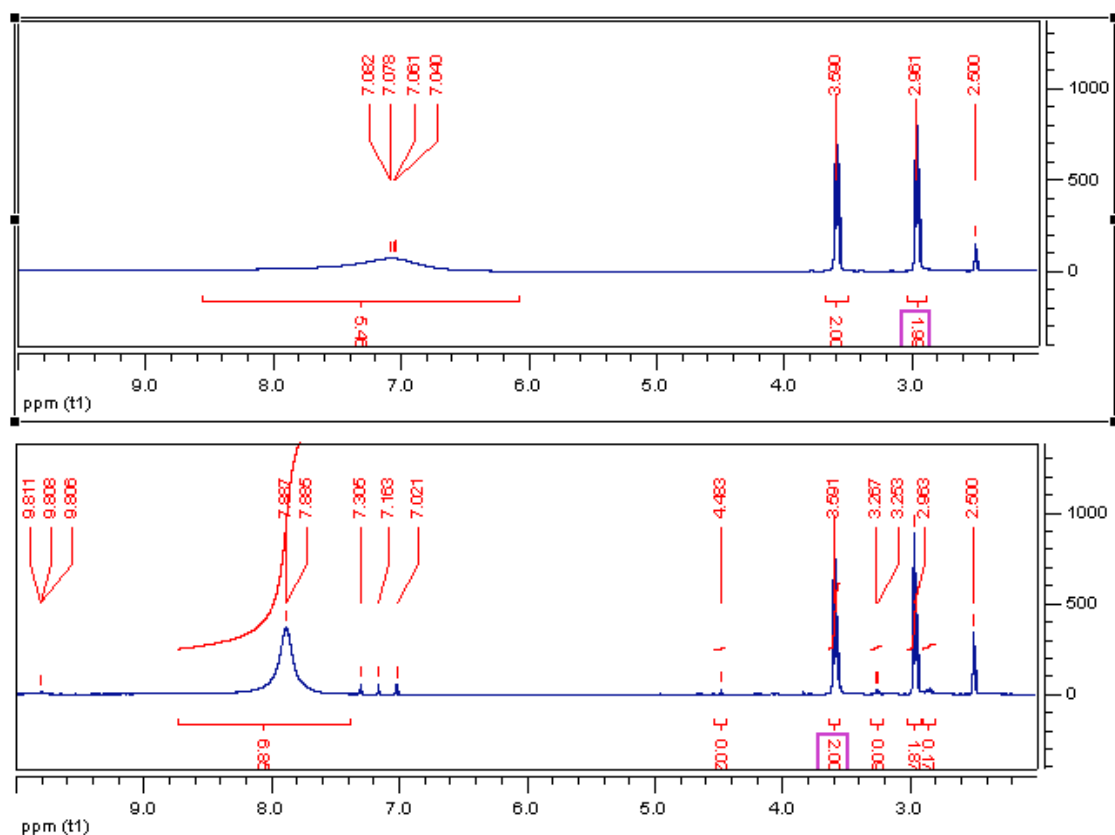
Figure A2: ^{1}H-NMR plot of 2-hydroxyethyl hydrazinium mononitrate (top) and dinitrate (bottom) salts; DMSO-d_6 360 MHz.

♦ The integration and downfield shift of amine/ammonium and hydroxy protons indicate the successful formation of the mono- and dicationic forms of the nitrate salts; where further downfield shifting is

observed for the dicationic salt (2+ formal charge, and more deshielding of electron density from the cationic protons).

♦ Small 1:1:1 triplet at δ ~ 7.1 ppm is indicative of the J_{N-H} spin-spin coupling that is typical for amine protons. Further J_{HN-CH} coupling is not observed due to peak broadening.

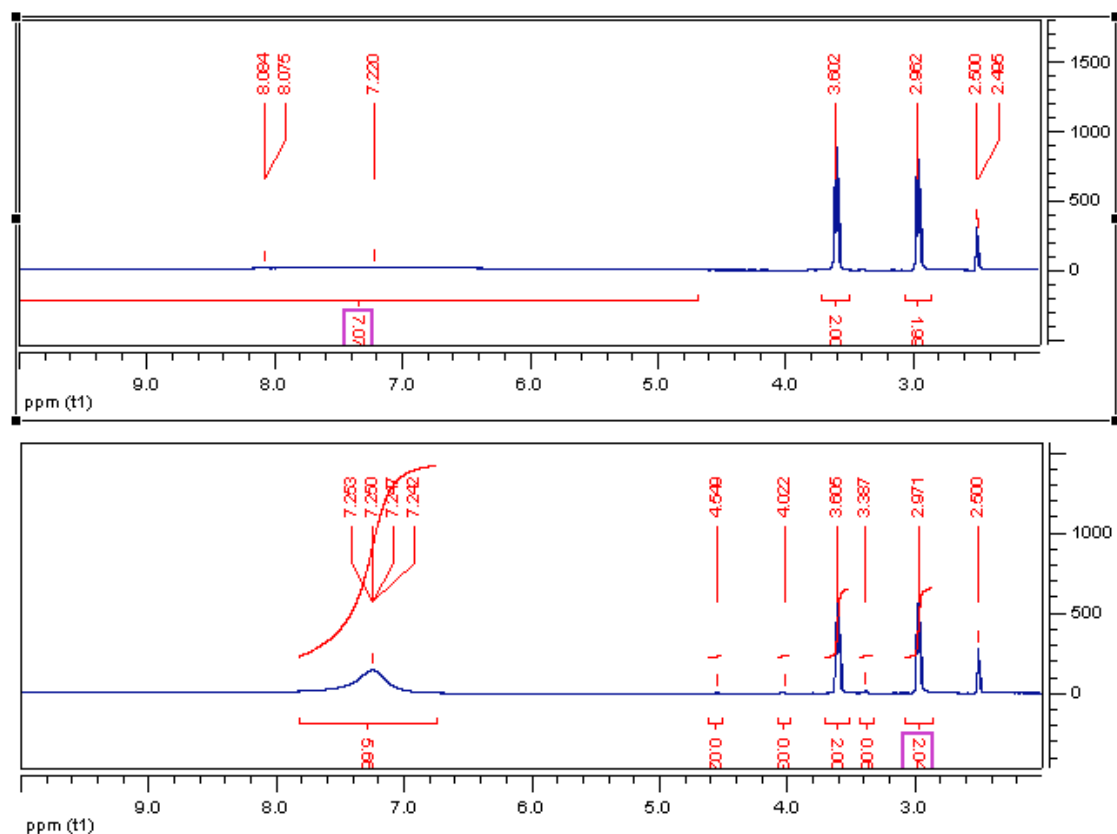**Figure A3:** **^{1}H-NMR plot of 2-hydroxyethyl hydrazinium monochloride (top) and dichloride (bottom) salts; DMSO-d_6 360 MHz.**

♦ The peak for N-H and O-H protons is expected to occur in the region between δ ~ 6-8 ppm. However, extensive broadening makes peak resolution difficult in the 1:1 chloride salt case. For the dication, the peak is less broadened and accurate for expected integrations of each proton signal.
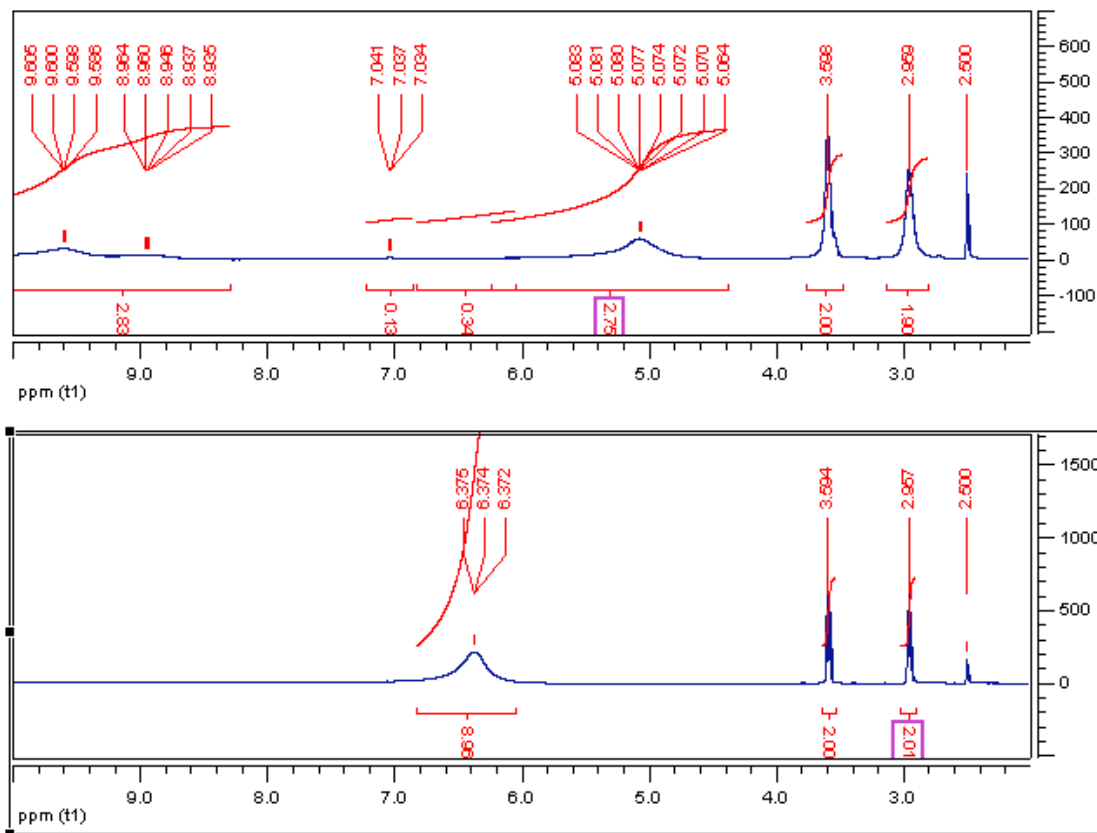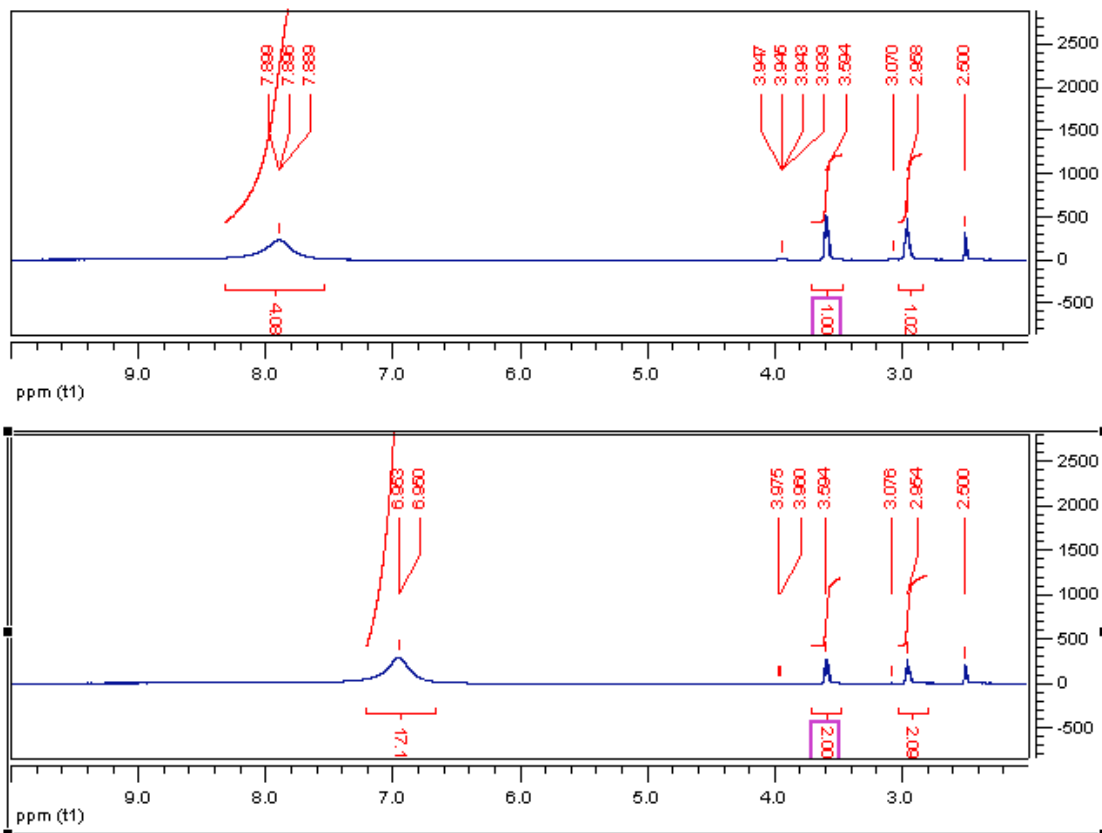
Figure A4: ^{1}H-NMR plot of 2-hydroxyethyl hydrazinium mono(tetrafluoroborate) (top) and di(tetrafluoroborate) (bottom) salts; DMSO-d_6 360 MHz.

- There is an unexplained downfield peak at $\delta \sim 9.5$ ppm, and the peak for the monocationic protons integrates to less than expected (2.75H(observed) vs. 5H(expected))
- 1:2 mixture for dicationic salt did not experience the above problems, and the obtained sample, however, the proton signal for –OH and ammonium/amine protons appears to be somewhat higher in integration than expected (~ 9H vs. 7H expected). Again, this might be attributed to the difficulty when integrating the broadened signal.

Figure A5: ^{1}H-NMR plot of 2-hydroxyethyl hydrazinium mono(hexafluorophosphate) (top) and di(hexafluorophosphate) (bottom) salts; DMSO-d_6 360 MHz.

◆ The peaks for amine/ammonium and hydroxy protons show a reverse of expected chemical shift for the hexafluorophosphate salts compared with the other spectra ($\delta_{monocation}$ = 7.896 ppm vs. $\delta_{dication}$ = 6.953 ppm).

Part B: Thermal Analysis (TGA / DSC / Thermal Stability):

◆ The thermal properties for the synthesized 2-OHEt-HY salts are summarized in the table below (Table 1B):

Table 1B: Thermal Data Collected for Mono- and Dicationic 2-OHEt Hydrazinium Salts

SALT/RATIO	TGA (^{o}C)†	DSC (^{o}C)‡	Thermal Stablility*
2-hydroxyethyl-hydrazine (neutral)	T_{onset} = 181.98 $T_{5\% dec}$ = 102.10 T_{dec} = 195.94	T_g = -72.11	- 88.1 % weight loss
2-OHEt hydrazinium nitrate; 1:1	T_{onset} = 214.10 $T_{5\% dec}$ = 193.63 T_{dec} = 259.67	T_g = -56.91	-23.8 % weight loss
2-OHEt hydrazinium nitrate; 1:2	T_{onset} = 91.51 $T_{5\% dec}$ = 62.71 T_{dec} = 101.01	T_g = -47.89	-43.8% weight loss
2-OHEt hydrazinium chloride; 1:1	T_{onset} = 223.19 $T_{5\% dec}$ = 171.15 T_{dec} = 251.33	T_g = -50.61	-8.8 % weight loss
2-OHEt hydrazinium chloride; 1:2	T_{onset} = 240.33 $T_{5\% dec}$ = 183.17	T_g = -49.37	-7.8 % weight loss

SALT/RATIO	TGA (^{o}C)†	DSC (^{o}C)‡	Thermal Stablility*
	T_{dec} = 282.18		
2-OHEt hydrazinium tetrafluoroborate; 1:1	T_{onset} = 198.49 $T_{5\% dec}$ = 192.79 T_{dec} = 310.59	T_g = -46.22	-7.1 % weight loss
2-OHEt hydrazinium tetrafluoroborate; 1:2	T_{onset} = 160.66 $T_{5\% dec}$ = 79.02 T_{dec} = 215.26	T_g = -55.49	-38.8 % weight loss
2-OHEt hydrazinium hexafluorophosphate; 1:1	T_{onset} = 106.56 $T_{5\% dec}$ = 119.21 T_{dec} = 114.67	T_g = -32.75	-40.2% weight loss (-29.2 % weight loss with sample dried at 60 ^{o}C for 12 hours)
2-OHEt hydrazinium hexafluorophosphate; 1:2	T_{onset} = 106.91 $T_{5\% dec}$ = 119.21 T_{dec} = 114.67	T_g = -33.46	- 41.5 % weight loss
2-OHEt hydrazinium bis(trifylamide); 1:1	T_{onset} = 162.57 $T_{5\% dec}$ = 143.75 T_{dec} = 183.03	T_g = -48.75	-17.5 % weight loss
2-OHEt hydrazinium bis(trifylamide); 1:2	T_{onset} = 158.12 $T_{5\% dec}$ = 156.12 T_{dec} = 178.34	T_g = -51.04	-12.2 % weight loss

† All TGA measurements were made on dynamic heating regime using a TGA model 2950 TA Instruments. Instrument under air atmosphere and samples limited to below 15 mg. Samples were first heated to 75 ^{o}C and kept at this temperature for 30 min to allow all remaining water to evaporate. Then the samples were heated at a rate of 5 ^{o}C min^{-1} from room temperature to 600 or 800 ^{o}C.
‡ DSC analysis was conducted on a TA Instruments Modulated DSC cooled with a liquid nitrogen cryostat, and data was collected at atmospheric pressure using 5-20 mg samples in sealed, pin-holed aluminum pans with caps. An empty pan was used as reference.
* Thermal stability tests were taken for samples by using ~10-20 mg samples with the TGA and setting to ramp at 5 ^{o}C min^{-1} to 75 ^{o}C and allowing isothermal for 24 hours.
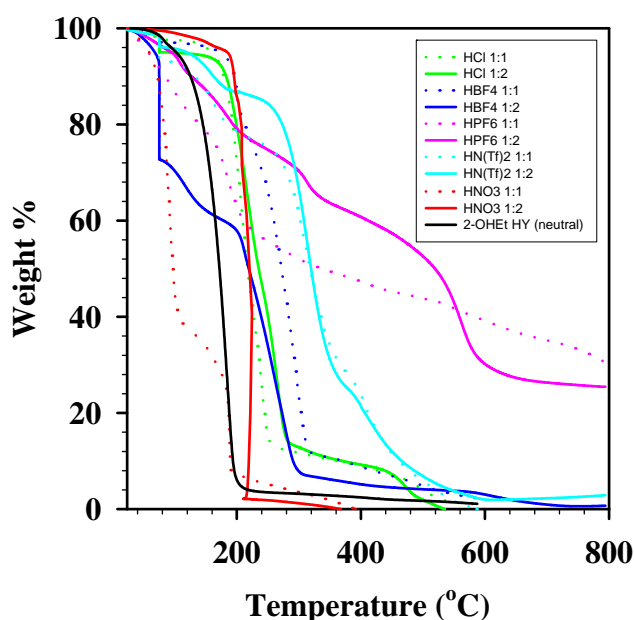

Figure 1B: Comparative TGA plot for the thermal decomposition of monocation (dotted lines) and dicationic (solid lines) salts of 2-hydroxyethyl hydrazine (black line, reference).

Thermal decomposition: Thermograviometric analysis (TGA) was utilized to identify the temperatures for decomposition (**T$_{dec}$**) and temperature for onset of decomposition (**T$_{onset}$**). In addition, the temperature at which

5 % of the material has thermally decomposed ($T_{5\% \text{ dec}}$) is included as a more accurate assessment of the real onset for thermal decomposition of the bulk material. Conditions for these analyses were to heat 5-15 mg of sample to 800 °C. The TGA plots (Figure 1B) provide a comparative view of how the series of synthesized salts behaved when undergoing thermal decomposition.

Thermal decomposition results discussion:

♦ Generally, the monocation for nitrate seems to be more stable than the dication as can be seen when noting the earlier onset of decomposition for the dication.
♦ The ratio of mass lost in the first and second decomposition steps of the dicationic nitrate might suggest the loss of (2) molecules of HNO_3.
♦ In general, the chloride salts (mono- and dicationic forms) demonstrated very good thermal stabilities, with quite a late onset of decomposition.
♦ Additionally, the decomposition of the chloride salts occurred with the majority of weight lost in the first step. A minor decomposition step can be observed near 450 °C.
♦ The BF_4^- salts both demonstrated a fairly direct decomposition near 200 °C, however.
♦ The explanation for differences in the onset of decomposition may be due to changes in the composition of the salt mixture that result from one or more of the following reason:
　　o Change in composition as a result of dynamic acid/base equilibrium where only one of the components present (acid or starting material) evaporates.
♦ PF_6^- salts were found to degrade immediately upon the start of TGA, even without the presence of an isothermal event.
♦ Both of the NTf_2^- salts were found to have (3) distinct decomposition events involved with the loss of weight.
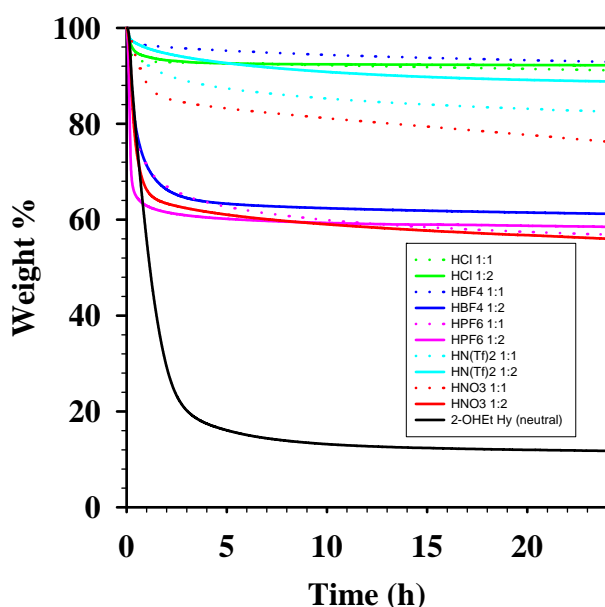

Figure 2B: Comparative TGA plots for the thermal stability of obtained monocationic (dotted lines) vs. dicationic (solid lines) salts of 2-hydroxyethyl hydrzazine (black line, reference).

Thermal Stability: The relative thermal stabilities of each salt is assessed by isothermic heating of a small sample on the TGA instrument for 24 hours @ 75 °C. The % weight loss of the sample is provided above in Table B1, and the comparative TGA plots for thermal stability are provided in Figure 2B. Conditions for theses analyses were as follows:

　　o Ramp of temperature by 5 °C/min to 75 °C.
　　o Isothermal heating for 24 hours.

Thermal Stability Data Discussion:

♦ The presence of an initial onset that varies to an arbitrary degree might suggest the possibility of dynamically changing composition due to the loss of either acid or starting material from evaporation (as mentioned earlier).
♦ Such confounding data beckons further investigation to probe into the cause for the early onset of decomposition in the isothermal data as collected.

*DSC Data (based on data summarized in Table B1)***:**
♦ Glass transitions are generally at higher temperatures compared with the parent HEH.
♦ All salts were recorded as room temperature ionic liquids with glass transitions <0 ^{o}C

Δ. Preliminary Conclusions and Future Directions:

♦ Work completed includes:
  o Synthesis of (10) HEH-based salts on 1.5 gram scale (Five 1:1 and five 1:2)
    ▪ Nitrates
    ▪ Chlorides
    ▪ Tetrafluoroborates
    ▪ Hexafluorophosphates
    ▪ Bistrifylamides
  o Synthesis of 2-OHEt-HY [NO$_3$] 1:1 salt on 5 gram scale
  o Characterization:
    ▪ ^{1}H-NMR
    ▪ TGA
    ▪ DSC
    ▪ Thermal Stability Testing
♦ The prototype of the 1:1 and 1:2 nitrate salts indicate higher thermal stability of the salts over the neutral HEH compound; TGA analysis indicates a more stable monocationic salt when compared with the dicationic dinitrate.
♦ Potential anion effects exist as well as speciation on phase transitions, as noted in the DSC data requires further attention.

REFERENCES

1 Canongia Lopes, J. N.; Padua, A. A. H. *J. Phys. Chem. B* **2006**, *110*, 19586.
2   Cadena, C.; Anthony, J. L.; Shah, J. K.; Morrow, T. I.; Brennecke, J. F.; Maginn, E. J. *J. Am. Chem. Soc.*, **2004**, *126*, 5300
3   Schmidt, M. W.; Baldridge, K. K.; Boatz, J. A.; Elbert, S. T.; Gordon, M. S.; Jensen, J. H.; Koseki, S.; Matsunaga, N.; Nguyen, K. A.; Su, S.; Windus, T. L.; Dupuis, M.; Montgomery, J. A. *J. Comp. Chem.* **1993**, *14*, 1347.
4   Boatz, J. A.; Gordon, M. S. *J. Phys. Chem.* **1989**, *93*, 1819
5   (a) Becke, A. D. J *Chem. Phys.* **1993**, *98*, 5648. (b) Becke, A. D. *J. Chem. Phys.* **1993**, *98*, 1372. (c) Lee, C.; Yang, W.; Parr, R. G. *Phys. Rev. B* **1988**, *37*, 785. (d) Godbout, N.; Salahub, D. R.; Andzelm, J.; Wimmer, E. *Can. J. Chem.* **1992**, *70*, 560.
6   Computational Chemistry Comparison and Benchmark Database. http://cccbdb.nist.gov/default.htm
7   Canongia Lopes, J. N.; Deschamps, J.; Padua, A. A. H. *J Phys. Chem. B* **2004**, *108*, 2038.
8   Brooks, B. R.; Bruccoleri, R. E.; Olafson, B. D.; States, D. J.; Swaminathan, S.; Karplus, M. *J. Comp. Chem.* **1983**, *4*, 187.
9   Phillips, J. C.; Braun, R.; Wang, W.; Gumbart, J.; Tajkhorshid, E.; Villa, E.; Chipot, C.; Skeel, R. D.; Kale, L.; Schulten, K. *J. Comp. Chem.* **2005**, *25*, 1781.
10 Breneman C. M.; Wiberg, K. B. *J. Comp. Chem.* **1990**, *11*, 361.
11 Canongia Lopes, J. N.; Padua, A. A. H. *J. Phys. Chem. B* **2004**, *108*, 16893
12 1. J. D. Martin, N. H. Lundstrum, R. S. Scheffe, Premixed Liquid Monopropellant Solutions and Mixtures, *US Pat.* 6984271, **2006**.
13 . Courthéoux, L.; Amariei, D.; Rossignol, S.; Kappenstein, C., Thermal and catalytic decomposition of HNF and HAN liquid ionic as propellants, *Appl. Catal. B* **2006,** *62*, 217-225.
14 . A. J. Brand, G. W. Drake, Energetic Hydrazinium Salts, US Pat. 6218577, **2001**.